Computer Methods and Programs in Biomedicine 219 (2022) 106737

Contents lists available at ScienceDirect

Computer Methods and Programs in Biomedicine

journal homepage: www.elsevier.com/locate/cmpb

Biomechanical analysis of the drilling parameters for early osteonecrosis of the femoral head

DaiZhu Yuan[a,b,c,1], ZhanYu Wu[b,c,1], Long Yang[b,c], Qiang Zou[b,c], DaWei Hua[b], ZiHao Zou[b], Chuan Ye[b,c,*]

[a] Medical College, Soochow University, Suzhou 215006, China
[b] Department of Orthopaedics, The Affiliated Hospital of Guizhou Medical University, Guiyang 550004, China
[c] Center for Tissue Engineering and Stem Cells, Guizhou Medical University, Guiyang 550004, China

ARTICLE INFO

Article history:
Received 16 September 2021
Revised 25 February 2022
Accepted 7 March 2022

Keywords:
Osteonecrosis
Core decompression
Finite element analysis
Parameter
Biomechanics

ABSTRACT

Background and objective: Core decompression is a surgical procedure commonly used to treat the early osteonecrosis of the femoral head. However, It is not known whether different drilling parameters affect postoperative biomechanical strength. This study aimed to analyze the mechanical stability of different drilling locations and diameters of core decompression using finite element analysis.

Methods: Finite element models were established based on computed tomography images obtained from five healthy participants, including the different drilling locations (Lesser trochanter: Above, Parallel, and Below) and diameters. Biomechanical parameters including stiffness and stress were evaluated under slow running loads.

Results: At the same drilling diameter, the femoral stiffness was highest ($p < 0.05$) in the Above group and lowest in the Below group, while the maximum equivalent stress of the entry area and the necrotic area was highest ($p < 0.05$) in the Below group and lowest in the Above group. With the increase of drilling diameters, the stiffness decreased and its decreased percentage comparing the preoperative: Above (1.06–8.82%), Parallel (2.51–13.61%), and Below (3.99–15.06%). The maximum equivalent stress of the entry area and necrotic area increased as the drilling diameter increased, and its increased percentage comparing the preoperative, for the entry area: Above (14.11–219.58%), Parallel (35.91–306.37%), and Below (46.12–240.98%); for the necrotic area: Above (13.64–114.69%), Parallel (29.37–187.76%), and Below (44.76–202.10%). The range of safety drilling parameters (SDP) was obtained (Below<9 mm, Parallel<11 mm, and Above<13 mm) by comparing the maximum equivalent stress of two areas and its yield strength. For patients of different sizes and normal bone mineral density (BMD), the maximum equivalent stress of the two areas did not exceed its yield strength using the range of SDP, except for the patients with abnormal BMD (Osteoporosis) or high body mass index (BMI≥28 kg/m^2).

Conclusions: The biomechanical properties of early osteonecrosis of the femoral head deceased with increasing drilling diameters parameters, especially at the location below the lesser trochanter. The SDP (Below<9 mm, Parallel<11 mm, and Above<13 mm) is a suitable reference for most patients to perform slow running postoperatively, while it may be not suitable for patients with osteoporosis or obesity.

1. Introduction

Osteonecrosis of the femoral head (ONFH) is a common yet refractory disease, largely caused by trauma, immunosuppressant abuse, and long-term alcohol abuse [1]. Inappropriate treatment can lead to the collapse of the femoral head and the destruction of hip joint function. Therefore, hip preservation treatment before the collapse of the femoral head in the early stage [2]. At present, the condition is mainly treated with core decompression of the femoral head or decompression combined with other methods, such as stem cell transplantation [3], platelet-rich plasma [4], porous tantalum rod implantation [5], and vascularized bone flap transplantation [6].

During core compression, a lateral trochanteric approach is made by drilling one single channel with a large-diameter core drill [7]. The lateral wall of the femur is cortical bone, which is denser than cancellous bone, with stronger resistance to compres-

* Corresponding author at: Department of Orthopaedics, The Affiliated Hospital of Guizhou Medical University, Guiyang 550004, China.
E-mail address: yechuanchina@hotmail.com (C. Ye).
[1] These authors contributed equally to this work.

https://doi.org/10.1016/j.cmpb.2022.106737
0169-2607/

sion and distortion, and thus is essential for the mechanical support of the entire body [8]. The core decompression damages the cortical bone on the lateral wall, causing damage to the original mechanical structure and a decline in its mechanical strength. Studies have shown that the integrity of the lateral wall of the trochanter is important for maintaining the biomechanical stability of the proximal femur [9]. Drilling holes at the different locations on the lateral wall results in changes in the mechanical strength of local bones and even increases the risk of fractures. It was reported that during the core decompression combined with tantalum rod implantation for early-stage osteonecrosis of the femoral head, subtrochanteric fracture occurred after surgery due to drilling below the lesser trochanter [10]. Cannulated screws were inserted into different locations on the lateral wall of the femoral trochanter in an inverted triangle arrangement for finite element analysis, the results showed that the upper location induced the lowest stress level while the lower location induced the highest stress level, and stress shielding occurred [11].

Although single-channel large-diameter drilling for core compression effectively removes the diseased and necrotic tissues from the femoral head, the structural bone is hollowed out, creating a cavity and causing changes and even concentration of local stress. As a result, the mechanical support of the subchondral bone is significantly weakened. When the fractures accumulate to exceed the capacity of bone repair, they can eventually cause the femoral head to collapse [12]. In order to minimize the effects on the biomechanical strength of the proximal femur, some have adopted the multiple small drilling technique [13]. The small-diameter decompression leaves the bony tissues connected between the holes, which has a smaller impact on the biomechanical performance than the single-channel large-diameter decompression does. Due to the small hole diameter, however, the technique serves as core compression alone but restricts combination with other methods to treat ONFH. There has been no theoretical support for whether it affects postoperative mechanical stability compared with the large-diameter drilling compression. For this reason, the conventional concept of hip fracture is still followed to avoid early weight-bearing activities, which fails to properly guide postoperative rehabilitation for patients [14]. At present, there have been few studies on whether the different drilling locations and diameters made on the lateral wall of the trochanter for single-channel core decompression permit slow running, and whether it affects the local biomechanical strength to increase the risk of fracture. Therefore, it is crucial to correctly evaluate the risk of fracture based on the different drilling parameters for core decompression.

In this study, the three-dimensional finite element method was used to analyze the stiffness and stress induced by the different drilling locations and diameters of core compression on the proximal femur under slow running loads. Then, the range of SDP that decreases the risk of femoral fracture and collapse of the necrotic area was obtained, which will provide orthopedic surgeons with the appropriate drilling parameters and guide the postoperative activity intensity for patients.

2. Materials and methods

2.1. Construction of three-dimensional (3D) femur model and early ONFH

Five healthy participants ranging in age from 20 to 60 years without any history of hip trauma, hormone use, and or long-term alcohol consumption were recruited for the present study (Table 1). Mimics software (Version 21.0, materialize, Leuven, Belgium) was used to develop five patient-specific femur models based on 0.625 mm thick computed tomography (CT) images (Fig. 1A, B). Then, we constructed the early ONFH, the necrosis area was determined based on the angles in the mid-coronal and mid-sagittal images of the femur head. Both angles were set at 100° corresponding to the extent of early ONFH (Fig. 1C) [15].

2.2. Construction of different core decompression models

One hundred and sixty finite element models for the different parameters of core decompression were constructed using 3-Matic software (Version 11.0, materialize, Leuven, Belgium). The drilling diameters ranged from 6 mm to 17 mm (without damaging the femoral neck cortical bone structure) and the drilling locations were above, parallel to, and below the lesser trochanter. The overall drilling parameters were obtained as follows: Lesser trochanter (Above): 6–15 mm, Lesser trochanter (Parallel): 6–17 mm, and Lesser trochanter (Below): 6–15 mm (Fig. 1D).

2.3. Finite element biomechanical analysis

The solid models were discretized into ten-node tetrahedral three-dimensional elements (solid 92), and the mesh size of the intact femur was determined by a convergence test of the construct stiffness (Fig. 2C). There were approximately 550,000 nodes (from 523,359 to 577,192) and 300,000 elements (from 286,898 to 323,765) in each model (Table 2). The apparent density (ρ), Young's modulus (E), and Poisson's ratio of each element were assigned based on the Hu value in the CT scans data according to the following formula [16] and previous studies [17] (Fig. 2A, B).

$$\rho\left(\mathrm{g/cm^3}\right) = 0.000968 \times \mathrm{HU} + 0.5$$

$$\text{If } \rho < 1.2\,\mathrm{g/cm^3};\ E = 2014\rho^{2.5}(\mathrm{MPa}),\ \ \nu = 0.2$$

$$\text{If } \rho > 1.2\,\mathrm{g/cm^3};\ E = 1763\rho^{3.2}(\mathrm{MPa}),\ \ \nu = 0.32$$

The necrotic bone was assumed to be linearly elastic, homogeneous, and isotropic. The moduli of elasticity were 332.9 MPa, and the Poisson's ratios were 0.3 [18]. All models were exported into ANSYS Workbench 2021 software (ANSYS, American) for further analysis. The distal end of the femur was fixed. The mechanical loads of slow running were assigned to the femoral head according to a previous study [19] (Fig. 3A, B).

2.4. Evaluation indicators

The femoral stiffness and maximum equivalent stress at the entry area and necrotic area were used to evaluate the biomechanical properties of early ONFH after core compression. Data extracted from the finite element models were primarily tested for normality using the Shapiro–Wilk test. A one-way ANOVA with Tukey's post hoc test was used to compare the means of the different groups for the mechanical data and an unpaired t-test was used for comparison between just two groups. $P < 0.05$ was statistical difference.

3. Results

3.1. Model validation

Fig. 2C showed the validation of the current study in terms of result convergence and construct stiffness. The construct stiffness was defined as the ratio of the femoral vertical displacement to the applied loads [20]. During validation of construct stiffness, the intact femur was subject to the same loads as in Koval's study (Cadaver test) [21]. Construct stiffness of the intact femur converged to 1238.24 ± 9.25 N/mm until the element size reached about 1 mm in this study. For the convergent stiffness, the error of our study and Koval's study(1230 N/mm) was only 0.67%. This indicates that good agreement was achieved and the intact femur was validated for further analyses.

Table 1
Baseline information.

Patients	Sex	Age	Height (cm)	Weight (kg)	BMI [a](kg^2/m)	FL [b](cm)	NSA (°)	FAA (°)	HU [c]
1	M	25	165	50	18.4	41.3	126.4	15.3	563.2
2	F	36	156	72	29.2	39.0	130.6	13.6	496.7
3	F	41	163	71	26.7	40.8	128.1	15.8	366.4
4	M	43	176	67	21.6	44.0	126.8	14.7	410.2
5	F	57	158	56	22.4	39.5	125.6	12.9	253.6

Abbreviations: BMI, body mass index; FL, femur length; NSA, femoral neck shaft angle; FAA, femoral anteversion angle.
[a] BMI can be divided into four categories: Underweight (<18.5 kg/m^2); Normal (18.5–23.9 kg/m^2); Overweight (24–27.9 kg/m^2); Obesity (≥ 28 kg/m^2).
[b] Femur length was defined as the distance from the center of the femoral head to the intercondylar notch.
[c] Hu indicates the average Hu value in the fitted ovoid region of the middle femoral neck. A Hu value above 262 can be used to confirm the absence of osteoporosis according to the previous article.

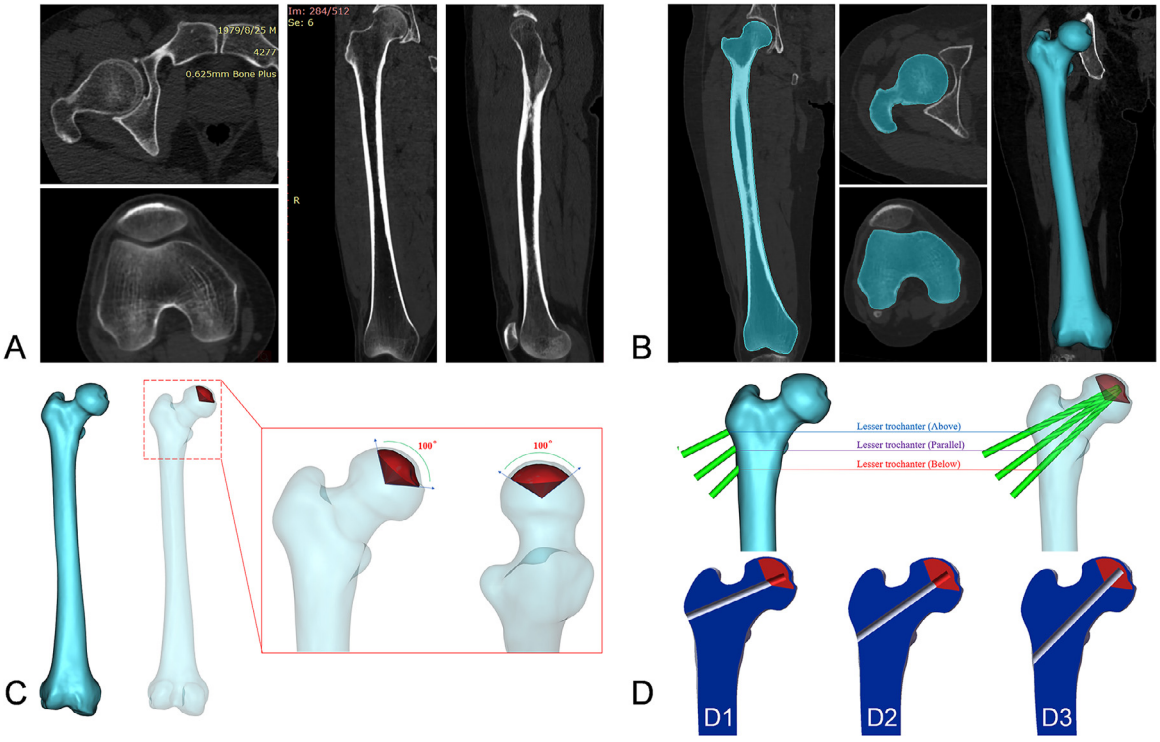

Fig. 1. (A) Computed tomography (CT) images of patients; (B) Construction of 3D femur model; (C) Construction of the early ONFH; (D) Construction of different core decompression models: (D1) Lesser trochanter (Above), (D2) Lesser trochanter (Parallel), (D3) Lesser trochanter (Below).

Table 2
Notes and elements of preoperative patients in this study.

	Patient1	Patient2	Patient3	Patient4	Patient5
Nodes	572,615	549,212	565,704	577,192	558,483
Elements	320,928	306,407	316,635	323,765	312,150

3.2. Construct stiffness

At the same location, as the drilling diameters increased, the femoral stiffness decreased comparing the preoperative (Fig. 4A). The preoperative femoral stiffness was 1242.96 ± 8.82 N/mm. The corresponding decreased stiffness ranges at three drilling locations were as follows respectively (including decreased percentage comparing the preoperative):1229.74–1133.33 N/mm (1.06–8.82%) for Above, 1211.70–1073.76 N/mm (2.51–13.61%) for Parallel, and 1193.41–1129.22 N/mm (3.99–15.06%) for Below (Table 4). Comparison of stiffness values at three drilling locations with the same diameter, Stiffness was highest ($p < 0.05$) in the Above group and lowest in the Below group: Lesser trochanter (Above)>Lesser trochanter (Parallel)>Lesser trochanter (Below). The stiffness values of three drilling positions were all decreased with increasing drilling diameter parameters and were statistically significant ($p < 0.05$) comparing the preoperative. However, for the drilling diameter of 6 mm at the lesser trochanter (Above), the postoperative stiffness value decreased compared with that before surgery and was no statistical significance ($p > 0.05$) (Fig. 5A). As can be seen from Table 3, for patients with osteoporosis or BMI≥28 kg/m^2 (Obesity), the postoperative stiffness was lower compared to other patients.

3.3. Stress of the entry area under slow running loads

With the drilling parameter increased, the maximum equivalent stress of the entry area increased compared to the preoperative (Fig. 4B). Preoperative stress values of the three drilling locations were as follows: 30.33 ± 4.59 MPa (Above), 38.96 ± 5.61 MPa (Parallel), and 49.37 ± 10.27 MPa (Below). Corresponding to the range of increased stress values (including increased percentage comparing preoperative): 34.61–96.93 MPa (14.11–219.58%) for Above, 52.95–158.32 MPa (35.91–306.37%) for Parallel, and 72.14–168.34 MPa (46.12–240.98%) for Below (Table 5). Comparison of

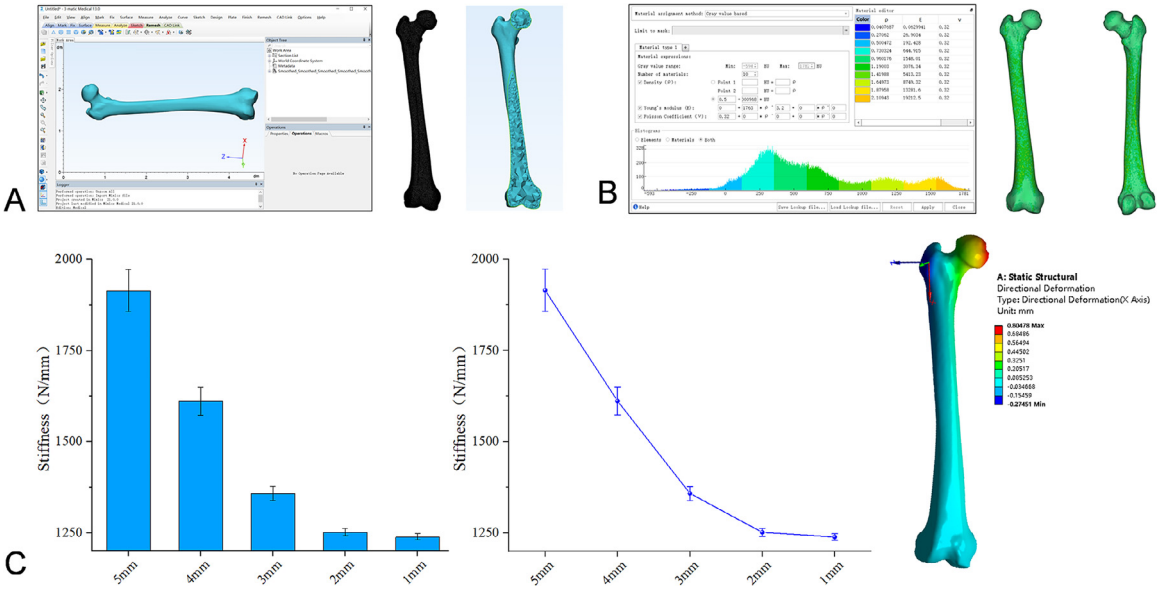

Fig. 2. (A) Division of volume mesh and face mesh; (B) Material properties based on the Hounsfield units from the CT scan data; (C) Model validation based on construct stiffness.

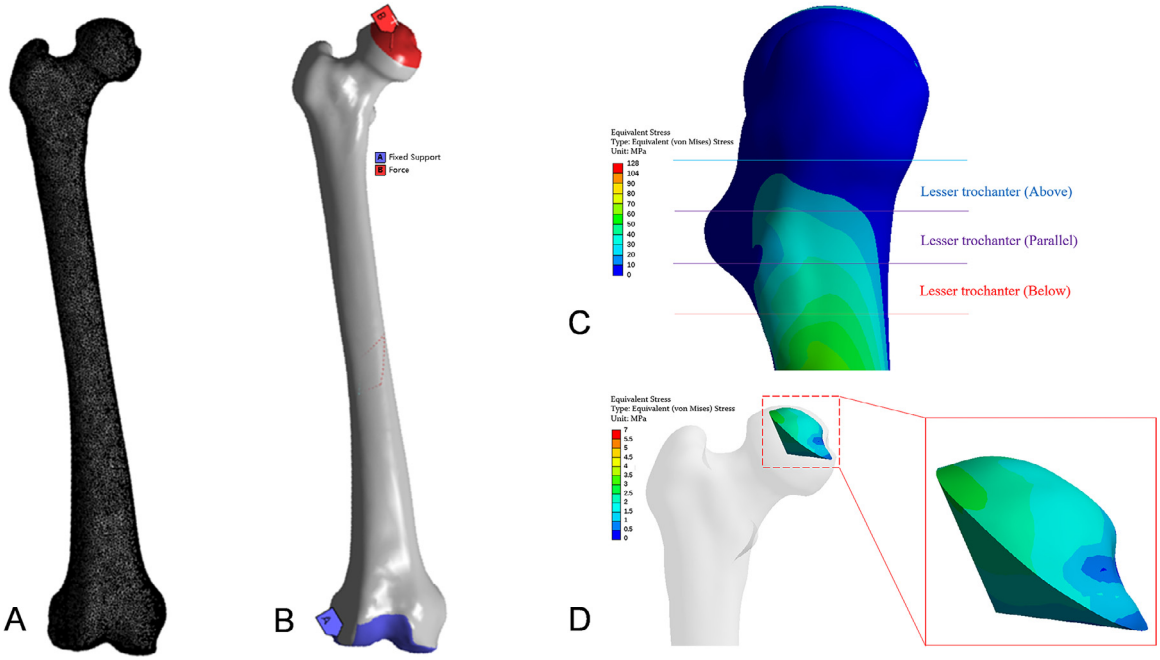

Fig. 3. (A) Mesh of the femur; (B) Boundary conditions; (C) Preoperative stress distribution of three drilling locations based on the lesser trochanter; (D) Preoperative stress distribution of the necrotic area.

the maximum equivalent stress at three drilling locations with the same diameter, the stress values of models were as follows: Below>Parallel>Above. The maximum equivalent stress was highest ($p < 0.05$) in the Below group and lowest in the Above group. As shown in Fig. 6 of the patient-3, The stress increased gradually and appeared concentration phenomenon at the entry area with the increase of the diameter parameters, especially at the location below the lesser trochanter. Diameter parameters corresponding to cortical bone yield strength (104 MPa [22]) of the entry area in three drilling locations were as follows: Below=9 mm, Parallel=12 mm (Fig. 4D), while at the lesser trochanter (Above), as the drilling diameters increased, the yield strength was not reached due to the diameter limitation. Therefore, SDP of the entry area was obtained: Below<9 mm and Parallel<12 mm. For patients with osteoporosis or BMI≥28 kg/m^2 (Obesity), the maximum equivalent stress was higher comparing other patients (Table 3).

3.4. Stress of the necrotic area under slow running loads

The maximum equivalent stress of the necrotic area increased compared to the preoperative as the drilling parameter increased (Fig. 4C). The preoperative stress value was 2.86 ± 0.20 MPa. The corresponding increased stress ranges at three drilling locations were as follows respectively (including increased percentage comparing the preoperative): 3.25–6.14 MPa (13.64–114.69%) for Above, 3.70–8.23 MPa (29.37–187.76%) for Parallel, and 4.14–

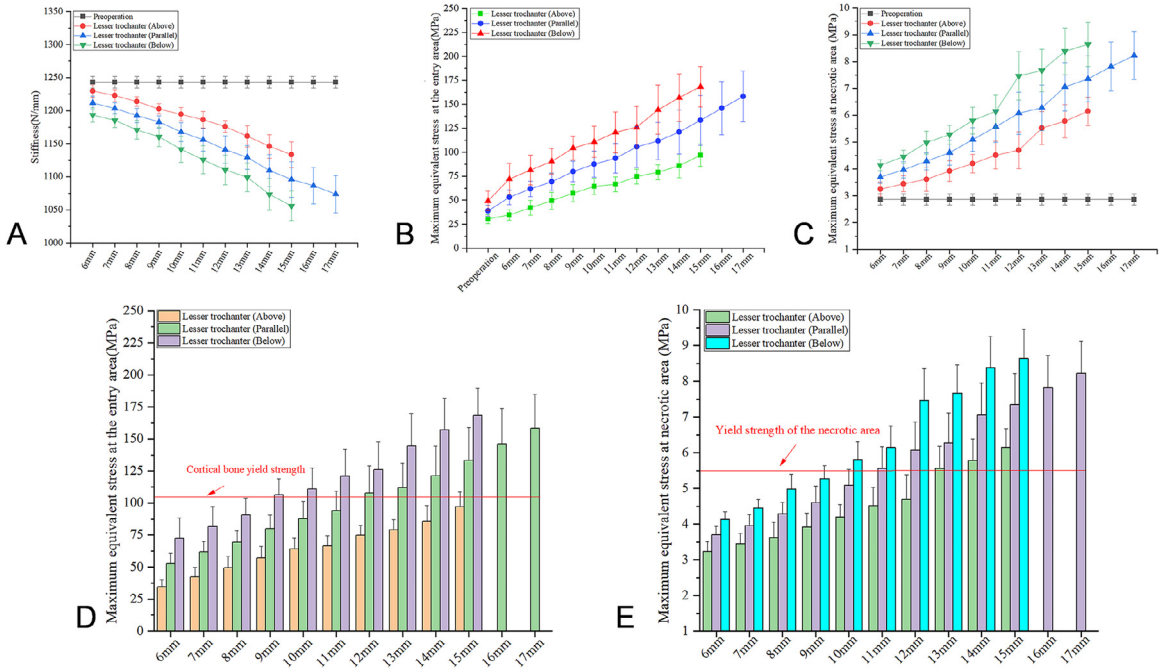

Fig. 4. (A) Femoral stiffness values of different diameters based on three drilling locations; (B) Maximum equivalent stress values of different diameters at the entry area based on three drilling locations; (C) Maximum equivalent stress values of different diameters at the necrotic area based on three drilling locations; (D) The range of SDP at the entry area: the maximum equivalent stress compared with cortical bone yield strength; (E) The range of SDP at the necrotic area: the maximum equivalent stress compared with yield strength.

8.64 MPa (44.76–202.10%) for Below (Table 6). Comparison of stress values at three drilling locations with the same diameter, the maximum equivalent stress was highest ($p < 0.05$) in the Below group and lowest in the Above group. Except for the drilling parameters of 6 mm at the lesser trochanter (Above), the maximum equivalent stress of three drilling positions were all increased and statistically significant ($p < 0.05$) comparing the preoperative (Fig. 5B). You can see this in Fig. 7, the maximum stress increased as the drilling parameter increased and increased most obviously at the location below the lesser trochanter. Diameter parameters corresponding to yield strength of the necrotic area (5.5 MPa [23]) at three drilling locations were as follows: Below=10 mm, Parallel=11 mm, and Above=13 mm (Fig. 4E). Therefore, the SDP of the necrotic area was as fellow: Below<10 mm, Parallel<11 mm, and Above<13 mm. This can be seen in Table 3, For patients with osteoporosis or BMI≥28 kg/m^2 (Obesity), the maximum equivalent stress was higher comparing patients with normal BMD.

3.5. SDP of core decompression under slow running loads

The overall SDP of three drilling locations was obtained (Below<9 mm, Parallel<11 mm, and Above<13 mm) by combining the SDP of two areas. As can be seen in Table 3, for the patients with osteoporosis (Patient-5), by applying the range of overall SDP, the maximum equivalent stress of the entry area and necrotic area corresponding to the three drilling positions was as fellow: for the entry area, 8 mm=106.38 MPa (Below), 10 mm=95.08 MPa (Parallel), and 12 mm=78.16 MPa (Above); for the necrotic area, 8 mm=5.16 MPa (Below) and 10 mm=5.54 MPa (Parallel) 12 mm=5.12 MPa (Above). The maximum equivalent stress of two locations (Below<9 mm and Parallel<11 mm) exceeded the yield strength. However, for the location (Below<13 mm), the corresponding maximum equivalent stress did not exceed the yield strength of the two areas, so the overall SDP at this location may be a suitable reference for patients with osteoporosis. In Tables 1 and 3, based on the overall SDP of three drilling locations, we compared the maximum equivalent stress in patients with different femoral sizes (short FL and long FL) and found that for patients with short FL and big weight (Patient-2: BMI>28.0, Obesity), the maximum stress values of three drilling locations all exceeded the yield strength of the two areas. We also performed detailed comparisons for patients with different geometric angle parameters of the proximal femur (NSA and FAA) and found that the maximum stress values of three drilling locations all did not exceed the yield strength of the two areas (Table 3), except for the patients with osteoporosis or BMI≥28 kg/m^2 (Obesity).

4. Discussion

In this study, the finite element method was used to compare the biomechanical effects of the different drilling locations and diameters of core decompression for the early ONFH after surgery. The results showed that as the drilling diameter increased, the resultant stress increased at the necrotic tissues and the entry area comparing the preoperative, while the femoral stiffness decreased. The biomechanical properties of early ONFH deceased with increasing drilling diameter parameters, especially at the location below the lesser trochanter.

BMD, an important indicator of bone strength, can reflect the degree of osteoporosis and is an important basis for predicting fracture risk [24]. In the present study, by comparing the effect of different BMD on the biomechanical properties of early ONFH, it was found that for patients with normal BMD, SDP of core decompression was a suitable reference for such patients to perform slow running after surgery, except for patients with BMI≥28 kg/m^2 (Obesity). Abnormal BMD (Osteoporosis) is a systemic bone disease in which bone density and bone strength decrease, mainly in the elderly [25]. Under the action of external forces, it is more likely to lead to an increased incidence of fracture. In this study, for patient-5 with osteoporosis, the maximum equivalent stress of the entry area and the necrotic area exceeded its yield strength value using the range of SDP, increasing the risk of postoperative fracture at

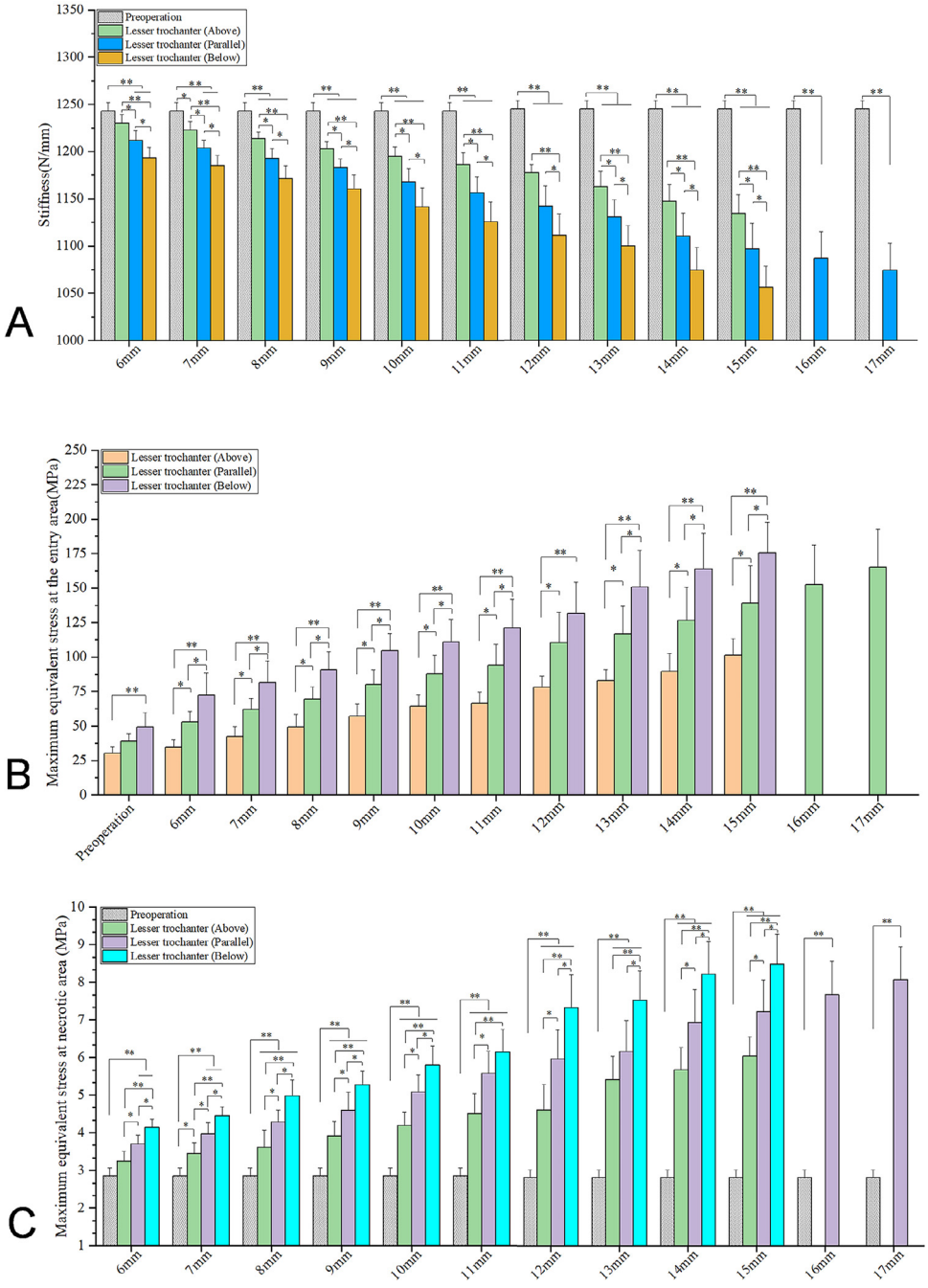

Fig. 5. (A) Femoral stiffness values of three drilling locations based on different diameters; (B) Maximum equivalent stress values of three drilling locations at the entry area based on different diameters; (C) Maximum equivalent stress values of three drilling locations at the necrotic area based on different diameters. The data are shown as mean ± standard deviation ($n = 5$), $^{*}p < 0.05$, $^{**}p < 0.01$.

the entry area and collapse at the necrosis area. By comparing the SDP of three locations, it was found that the SDP of two locations (Below<9 mm and Parallel<11 mm) was not suitable for patients with osteoporosis. However, the SDP of location (Above<13 mm) can be used as a suitable reference for such patients to perform slow running postoperatively. It is speculated that the drilling location of core decompression is related to the concentration area of stress in the proximal femur [26]. Studies have shown that at the proximal end of the femur, from the top down near the lesser trochanter and even below the lesser trochanter, the stress gradually increases, and even the stress concentration phenomenon occurs [27]. In this study, compared with the other two drilling locations (Below and Parallel), the drilling location (Above) was located above the lesser trochanter and far away from the stress concentration area, so the same mechanism also applies to our research.

By comparing the effect of patients with different sizes (FL, NSA, and FAA) on the biomechanical properties of early ONFH, it was found that SDP of core decompression was a suitable reference for most patients to perform slow running after surgery, except for patients with short FL and big weight (Patient-2: BMI>28.0, Obesity). The FL is in some way indicative of the patient's height [28] and can be explained by BMI. The BMI is determined by weight and height and is positively correlated with weight, while negatively correlated with height [29]. The results showed that for patients with normal BMD and approximate weight, the maximum

Table 3
The stiffness (N/mm) and the maximum equivalent stress (MPa) of different parameters at the entry area and the necrotic area in this study.

Models			6 mm	7 mm	8 mm	9 mm	10 mm	11 mm	12 mm	13 mm	14 mm	15 mm	16 mm	17 mm
		Stiffness	1244.31	1236.17	1223.96	1214.71	1210.14	1205.79	1189.47	1181.08	1165.19	1156.98		
	Above	Entry	27.68	33.64	39.78	46.95	54.56	57.35	65.75	69.86	71.95	83.33		
		Necrotic	2.88	3.12	3.11	3.51	3.73	3.83	3.84	4.89	5.11	5.61		
		Stiffness	1227.32	1216.27	1207.12	1196.82	1186.84	1176.17	1164.55	1145.11	1131.47	1122.92	1115.78	1102.29
1	Parallel	Entry	44.18	53.14	57.88	65.95	71.56	77.15	82.65	93.56	98.25	106.78	115.82	127.23
		Necrotic	3.40	3.62	3.85	3.94	4.69	4.94	5.33	5.24	5.81	6.21	6.53	6.98
		Stiffness	1208.84	1200.74	1189.49	1180.57	1165.22	1150.82	1137.67	1119.62	1098.23	1077.67		
	Below	Entry	51.18	62.14	73.88	89.65	92.56	96.75	100.23	108.85	123.45	141.93		
		Necrotic	3.83	4.16	4.61	4.85	5.26	5.38	6.11	6.62	7.20	7.52		
		Stiffness	1220.14	1213.58	1205.87	1194.54	1183.38	1173.39	1166.41	1137.56	1117.09	1105.02		
	Above	Entry	41.65	51.79	60.79	69.96	75.35	76.48	86.08	90.45	105.09	110.89		
		Necrotic	3.58	3.81	4.02	4.37	4.59	5.23	5.59	6.41	6.46	6.88		
		Stiffness	1201.31	1193.64	1179.78	1172.37	1148.79	1130.32	1111.67	1105.67	1075.77	1055.65	1044.31	1029.29
2	Parallel	Entry	63.15	71.29	80.89	94.96	106.76	113.25	132.99	137.62	149.29	164.85	178.63	188.18
		Necrotic	3.99	4.33	4.65	5.07	5.59	6.22	7.03	7.18	7.97	8.35	8.89	9.37
		Stiffness	1181.87	1173.83	1155.44	1143.61	1117.34	1098.52	1082.69	1071.69	1041.63	1028.81		
	Below	Entry	90.15	95.67	101.36	111.83	132.23	145.66	151.42	172.59	183.89	193.87		
		Necrotic	4.39	4.77	5.63	5.67	6.33	6.82	8.47	8.56	9.38	9.52		
		Stiffness	1233.06	1227.13	1217.52	1204.29	1198.25	1190.24	1177.96	1168.56	1152.98	1141.96		
	Above	Entry	31.44	37.36	43.03	51.45	58.47	60.36	70.78	75.46	79.87	88.34		
		Necrotic	3.11	3.23	3.35	3.65	3.97	4.32	4.33	5.09	5.19	5.69		
		Stiffness	1216.06	1204.95	1197.75	1187.12	1172.06	1165.73	1153.71	1142.65	1126.46	1109.68	1098.54	1085.25
3	Parallel	Entry	47.14	55.06	63.33	74.65	81.67	85.36	89.88	95.36	99.37	108.45	120.85	136.75
		Necrotic	3.55	3.71	4.08	4.41	4.91	5.21	5.41	5.62	6.55	6.89	7.46	7.86
		Stiffness	1199.91	1190.34	1182.03	1168.67	1155.84	1138.15	1123.67	1114.85	1091.56	1070.31		
	Below	Entry	62.14	71.39	82.33	96.85	98.67	102.06	108.75	129.86	141.57	154.14		
		Necrotic	4.08	4.31	4.68	5.05	5.35	5.64	7.11	7.15	7.85	8.08		
		Stiffness	1227.45	1220.74	1211.85	1202.6	1192.68	1183.86	1175.34	1162.75	1149.29	1138.74		
	Above	Entry	34.61	39.63	47.51	55.36	64.38	67.13	73.06	77.59	83.84	95.78		
		Necrotic	3.27	3.41	3.45	3.78	4.28	4.45	4.61	5.37	5.88	6.12		
		Stiffness	1208.54	1204.15	1193.45	1181.06	1170.25	1157.37	1146.08	1139.19	1120.82	1108.54	1098.46	1087.24
4	Parallel	Entry	53.11	61.13	68.96	79.36	83.38	85.93	99.96	106.45	119.47	133.78	147.63	159.48
		Necrotic	3.72	3.98	4.38	4.61	4.72	5.31	5.84	6.32	7.13	7.32	7.78	8.24
		Stiffness	1190.99	1182.54	1166.47	1159.13	1143.27	1130.71	1114.48	1108.75	1079.95	1067.47		
	Below	Entry	71.11	80.13	88.68	101.86	109.12	122.96	128.12	147.78	159.34	167.38		
		Necrotic	4.19	4.44	4.83	5.21	5.78	6.41	7.71	7.82	8.51	8.98		
		Stiffness	1223.72	1215.65	1208.91	1197.56	1188.46	1177.45	1170.34	1156.53	1144.97	1123.95		
	Above	Entry	37.68	48.39	56.12	62.25	69.08	71.36	78.16	82.61	88.48	106.32		
		Necrotic	3.39	3.68	4.14	4.28	4.42	4.75	5.12	5.86	6.25	6.42		
		Stiffness	1205.29	1198.28	1184.77	1177.05	1160.28	1150.71	1129.08	1114.88	1092.42	1082.43	1075.67	1064.74
5	Parallel	Entry	57.18	68.89	75.22	84.75	95.08	106.92	122.45	126.14	139.75	152.26	167.36	179.96
		Necrotic	3.85	4.18	4.49	5.01	5.54	6.19	6.78	7.02	7.83	8.02	8.42	8.68
		Stiffness	1185.45	1178.41	1161.82	1149.64	1126.11	1110.24	1092.88	1079.87	1055.79	1034.84		
	Below	Entry	86.12	98.23	106.38	121.93	122.17	136.68	142.23	162.79	176.43	184.39		
		Necrotic	4.23	4.59	5.16	5.61	6.29	6.47	7.92	8.21	8.97	9.12		

Table 4
The stiffness of different parameters and reduced percentage comparing the preoperation (Mean, N/mm).

Items	Lesser trochanter (Above)	Lesser trochanter (Parallel)	Lesser trochanter(Below)
Preoperation	1242.96		
6 mm	1229.74 (1.06%)	1211.70 (2.51%)	1193.41 (3.99%)
7 mm	1222.65 (1.63%)	1203.46 (3.18%)	1185.17 (4.65%)
8 mm	1213.62 (2.36%)	1192.57 (4.05%)	1171.05 (5.79%)
9 mm	1202.74 (3.24%)	1182.88 (4.83%)	1160.32 (6.65%)
10 mm	1194.58 (3.89%)	1167.64 (6.06%)	1141.56 (8.16%)
11 mm	1186.15 (4.57%)	1156.06 (6.99%)	1125.69 (9.43%)
12 mm	1175.90 (5.39%)	1141.02 (8.20%)	1110.28 (10.67%)
13mm	1161.30 (6.57%)	1129.50 (9.13%)	1098.96 (11.59%)
14 mm	1145.90 (7.81%)	1109.39 (10.75%)	1135.30 (13.64%)
15 mm	1133.33 (8.82%)	1095.84 (11.84%)	1129.22 (15.06%)
16 mm		1086.55 (12.58%)	
17 mm		1073.76 (13.61%)	

Table 5
The maximum equivalent stress of different parameters at the entry area and increased percentage comparing preoperation (Mean, MPa).

Items	Lesser trochanter (Above)	Lesser trochanter (Parallel)	Lesser trochanter (Below)
Preoperation	30.33	38.96	49.37
6 mm	34.61 (14.11%)	52.95 (35.91%)	72.14 (46.12%)
7 mm	42.16 (39.00%)	61.90 (58.88%)	81.51 (65.10%)
8 mm	49.45 (63.04%)	69.26 (77.77%)	90.53 (83.37%)
9 mm	57.19 (88.56%)	79.93 (105.16%)	104.42 (111.50%)
10 mm	64.37 (112.23%)	87.69 (125.08%)	110.95 (124.73%)
11 mm	66.54 (119.39%)	93.72 (140.55%)	120.82 (144.72%)
12 mm	74.77 (146.52%)	105.59 (171.02%)	126.15 (155.52%)
13 mm	79.19 (161.09%)	111.83 (187.04%)	144.37 (192.42%)
14 mm	85.85 (183.05%)	121.23 (211.17%)	156.94 (217.89%)
15 mm	96.93 (219.58%)	133.22 (241.94%)	168.34 (240.98%)
16 mm		146.06 (274.90%)	
17 mm		158.32 (306.37%)	

equivalent stress of the short FL at two areas increased compared with that of the long FL, and the structural stiffness of the femur decreased, reducing the postoperative mechanical strength. Previous studies have shown that under the same load, larger objects are more conducive to uniform distribution of overall stress and avoid stress concentration [30]. In this study, for patients with long FL (large femur), the maximum equivalent stress of the entry area and the necrotic area was lower than that of the small FL (small femur) with the same drilling diameter parameters. Therefore, the same mechanism also applies to our research. The nor-

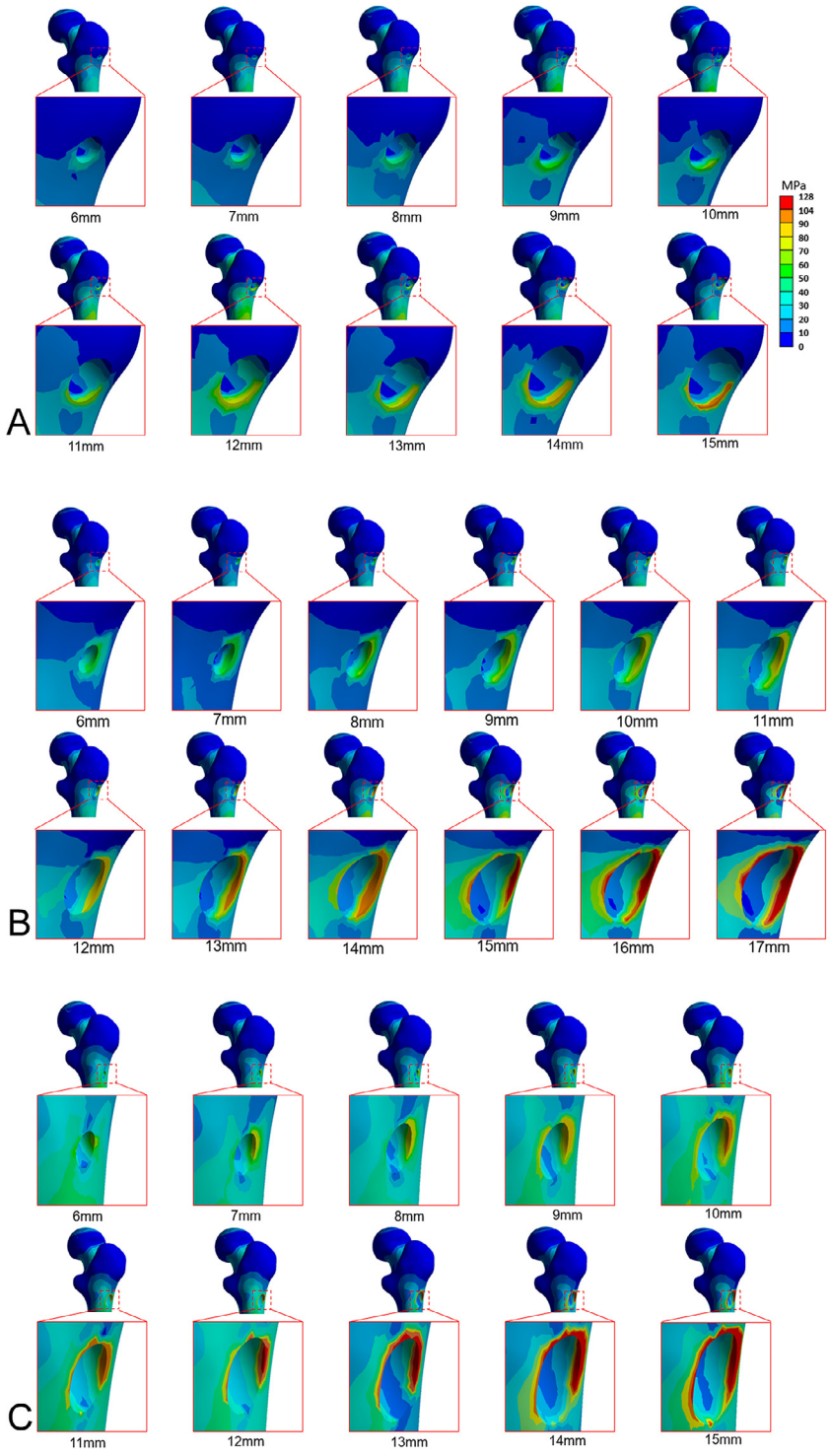

Fig. 6. Stress distribution of different diameters at the entry area for patient-3: (A) Lesser trochanter (Above); (B) Lesser trochanter (Parallel); (C) Lesser trochanter (Below).

mal conduction of load force is transmitted from the femoral head to the distal end of the femur [31]. Core decompression results in an uneven distribution of force transmitted from the femoral head compared to normal force transmission due to damage to the normal anatomical bone structure of the proximal femur, as well as changes in the overall stress distribution. In this study, the stress cloud map showed that the preoperative stress distribution on the femoral lateral wall was uniform. The stress was mainly distributed in the entry area after surgery, and the stress concentration phenomenon occurs as the drilling diameters increased. Under the same load, the small femur needs to bear more stress, and the change of stress distribution and concentration phenomenon were more obvious than that of the large femur. For patients with short FL and big weight (BMI>28.0, Obesity), the stress values of three drilling locations all exceeded the yield strength of the two areas using the range of SDP. Therefore, SDP was not suitable for patients with obesity.

The special geometric structure of the femoral neck can make it produce different elastic deformations with pressure directions under loads, so it can withstand larger stress and deformation

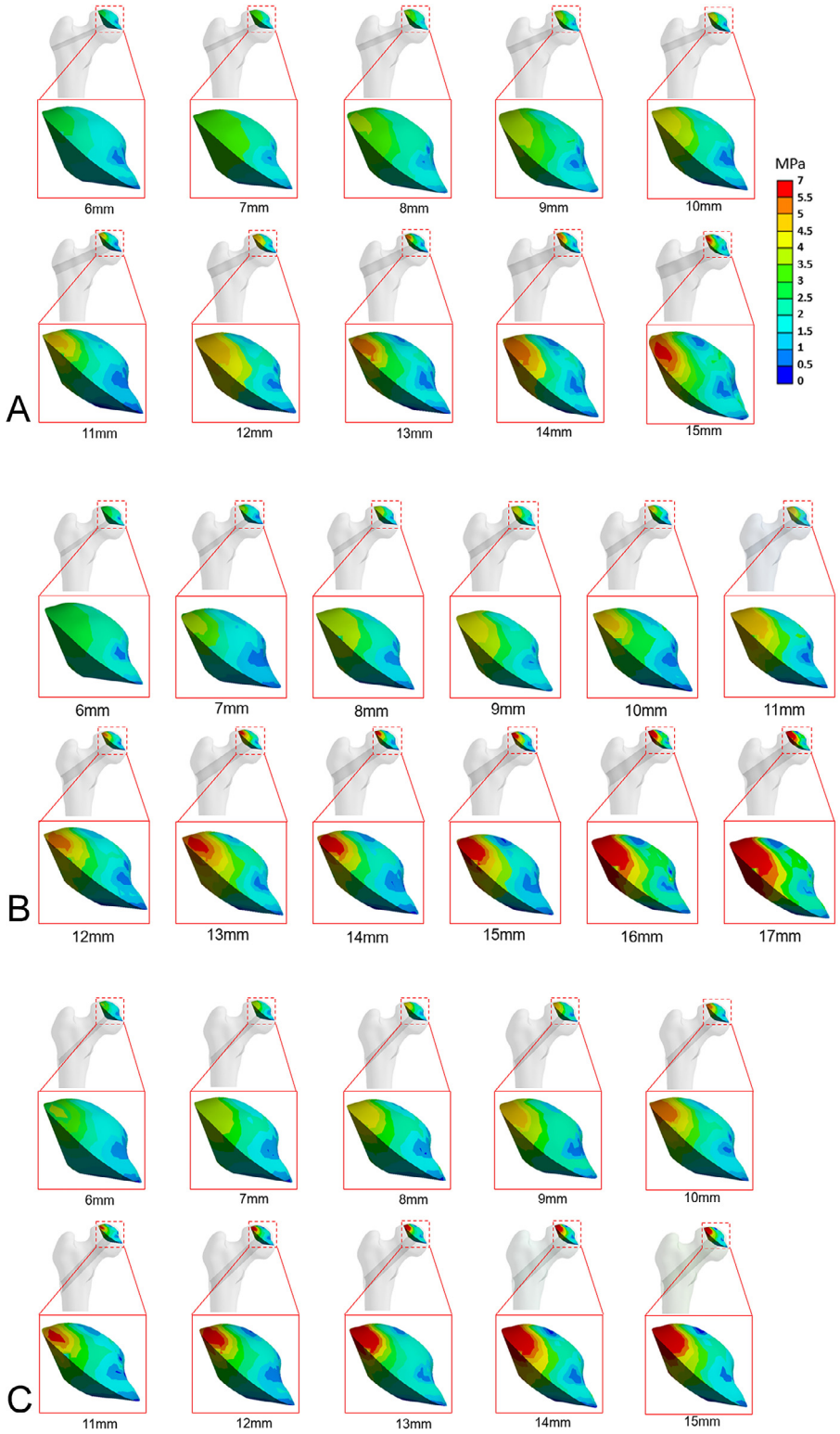

Fig. 7. Stress distribution of different diameters at the necrotic area for patient-3: (A) Lesser trochanter (Above); (B) Lesser trochanter (Parallel); (C) Lesser trochanter (Below).

[32]. Studies have shown that larger or smaller FAA can affect the biomechanical distribution of the proximal femur, the stress concentration in the proximal femur gradually shifted from the femoral calcar to the contact area between the femoral head and the femoral neck during the change of FAA [33]. NSA is an important risk factor for predicting hip fracture independent of BMD [34], the load transmitted from the body to the femoral head can be decomposed into two components after transformation, one of which is perpendicular to the femoral neck and related to the NSA, which is that the larger the NSA, the smaller the vertical component, the more difficult to fracture, on the contrary, the more prone to fracture [35]. The results of this study showed that excluding patients with BMI$\geq$28 kg/m^2 (Obesity) or osteoporosis, patients with different FAA and NSA could adapt to the range of SDP.

Table 6
The maximum equivalent stress of different parameters at the necrotic area and increased percentage comparing preoperation (Mean, MPa).

Items	Lesser trochanter (Above)	Lesser trochanter (Parallel)	Lesser trochanter (Below)
Preoperation	2.86		
6 mm	3.25 (13.64%)	3.70 (29.37%)	4.14 (44.76%)
7 mm	3.45 (20.63%)	3.96 (38.46%)	4.45 (55.59%)
8 mm	3.61 (26.22%)	4.29 (50.00%)	4.98 (74.13%)
9 mm	3.92 (37.06%)	4.61 (61.19%)	5.28 (84.62%)
10 mm	4.20 (46.85%)	5.09 (77.97%)	5.80 (102.80%)
11 mm	4.52 (58.04%)	5.57 (94.76%)	6.14 (114.69%)
12 mm	4.70 (64.34%)	6.08 (112.59%)	7.46 (160.84%)
13 mm	5.52 (93.01%)	6.28 (119.58%)	7.67 (168.18%)
14 mm	5.78 (102.10%)	7.06 (146.85%)	8.38 (193.01%)
15 mm	6.14 (114.69%)	7.36 (157.34%)	8.64 (202.10%)
16 mm		7.82 (173.43%)	
17 mm		8.23 (187.76%)	

Unfortunately, the FAA and NSA of the patients in this study were all within the normal range. However, whether a larger or smaller FAA and NSA can also adapt to the SDP of core decompression needs further study and verification.

The present study possesses some limitations. First, all material properties were assumed to be isotropic, linearly elastic, and homogeneous. In addition, we ignored the soft tissue surrounding the proximal femur. Despite these limitations, our findings may aid orthopedic surgeons in selecting the most appropriate drilling parameters of core compression.

5. Conclusions

Our findings indicate that the biomechanical properties of early ONFH decreased with the increase of drilling diameters, and the mechanical strength decreased most obviously at the location below the lesser trochanter. The maximum equivalent stress of the entry area and necrotic area increased as the drilling diameter increased, while the femoral stiffness decreased. The SDP (Below<9 mm, Parallel<11 mm, and Above<13 mm) is a suitable reference for most patients to perform slow running postoperatively, while it may be not suitable for patients with osteoporosis or obesity.

Ethics approval

This study conforms to the provisions of the Declaration of Helsinki and has been reviewed and approved by the Institutional Review Board of the Affiliated Hospital of Guizhou Medical University.

Declaration of Competing Interest

There are no conflicts of interest of all authors.

Acknowledgments

We thank Drs. ShunEn Xu, YuHu Zhou, and Xin Wu for their academic support. This study was supported by the Department of Science and Technology of Guizhou Province (LC [2021]003, [2020]4Y137, [2020]6013), the Health Commission of Guizhou Province (gzwkj2021-249), and the Science and Technology Bureau of Guiyang city ([2019]9-1-3).

Supplementary materials

Supplementary material associated with this article can be found, in the online version, at doi:10.1016/j.cmpb.2022.106737.

References

[1] W. Fu, B. Liu, B. Wang, D. Zhao, Early diagnosis and treatment of steroid-induced osteonecrosis of the femoral head, Int. Orthop. 43 (5) (2019) 1083–1087.
[2] B. Atilla, S. Bakırcıoğlu, A.J. Shope, J. Parvızı, Joint-preserving procedures for osteonecrosis of the femoral head, EFORT Open Rev. 4 (12) (2020) 647–658.
[3] Z.Y. Wu, Q. Sun, M. Liu, B.E. Grottkau, Z.X. He, Q. Zou, C. Ye, Correlation between the efficacy of stem cell therapy for osteonecrosis of the femoral head and cell viability, BMC Musculoskelet. Disord. 21 (1) (2020) 55.
[4] A.K. Aggarwal, K. Poornalingam, A. Jain, M. Prakash, Combining platelet-rich plasma instillation with core decompression improves functional outcome and delays progression in early-stage avascular necrosis of femoral head: a 4.5- to 6-year prospective randomized comparative study, J. Arthroplast. 36 (1) (2021) 54–61.
[5] K. Peng, Y. Wang, J. Zhu, C. Li, Z. Wang, Repair of non-traumatic femoral head necrosis by marrow core decompression with bone grafting and porous tantalum rod implantation, Pak. J. Med. Sci. 36 (6) (2020) 1392–1396.
[6] S. Popere, S.S. Shinde, R. Patel, A. Kulkarni, A cross sectional study of outcomes of muscle pedicle grafting in neck of femur fractures and avascular necrosis of femoral head, Injury 51 (7) (2020) 1622–1625.
[7] T.P. Pierce, J.J. Jauregui, R.K. Elmallah, C.J. Lavernia, M.A. Mont, J. Nace, A current review of core decompression in the treatment of osteonecrosis of the femoral head, Curr. Rev. Musculoskelet. Med. 8 (3) (2015) 228–232.
[8] I. Fleps, H. Bahaloo, P.K. Zysset, S.J. Ferguson, H. Pálsson, B. Helgason, Empirical relationships between bone density and ultimate strength: a literature review, J. Mech. Behav. Biomed. Mater. 110 (2020) 103866.
[9] Y. Gotfried, Integrity of the lateral femoral wall in intertrochanteric hip fractures: an important predictor of a reoperation, J. Bone Jt. Surg. Am. 89 (11) (2007) 2552–2553.
[10] B.M. Stronach, J.N. Duke, S.D. Rozensweig, R.L. Stewart, Subtrochanteric femur fracture after core decompression and placement of a tantalum strut for osteonecrosis of the femoral head, J. Arthroplast. 25 (7) (2010) 1168.e5–1168.e7.
[11] E. Sensoz, F.M. Özkal, V. Acar, F. Cakir, Finite element analysis of the impact of screw insertion distal to the trochanter minor on the risk of iatrogenic subtrochanteric fracture, Proc. Inst. Mech. Eng. H 232 (8) (2018) 807–818.
[12] C. Wang, H. Meng, Y. Wang, B. Zhao, C. Zhao, W. Sun, Y. Zhu, B. Han, X. Yuan, R. Liu, X. Wang, A. Wang, Q. Guo, J. Peng, S. Lu, Analysis of early stage osteonecrosis of the human femoral head and the mechanism of femoral head collapse, Int. J. Biol. Sci. 14 (2) (2018) 156–164.
[13] Y. Tan, H. He, Z. Wan, J. Qin, Y. Wen, Z. Pan, H. Wang, L Chen, Study on the outcome of patients with aseptic femoral head necrosis treated with percutaneous multiple small-diameter drilling core decompression: a retrospective cohort study based on magnetic resonance imaging and equivalent sphere model analysis, J. Orthop. Surg. Res. 15 (1) (2020) 264.
[14] T. Kuru, H.A. Olçar, Effects of early mobilization and weight bearing on postoperative walking ability and pain in geriatric patients operated due to hip fracture: a retrospective analysis, Turk. J. Med. Sci. 50 (1) (2020) 117–125.
[15] K.H. Koo, R. Kim, Quantifying the extent of osteonecrosis of the femoral head. A new method using MRI, J. Bone Jt. Surg. 77 (6) (1995) 875–880 Br.
[16] E. Reina-Romo, J. Rodríguez-Vallés, J.A. Sanz-Herrera, In silico dynamic characterization of the femur: physiological versus mechanical boundary conditions, Med. Eng. Phys. 23 (2018) S1350–S4533.
[17] D. Jiang, S. Zhan, L. Wang, L.L. Shi, M. Ling, H. Hu, W. Jia, Biomechanical comparison of five cannulated screw fixation strategies for young vertical femoral neck fractures, J. Orthop. Res. 39 (8) (2021) 1669–1680.
[18] T.D. Brown, M.E. Way, A.B. Ferguson, Mechanical characteristics of bone in femoral capital aseptic necrosis, Clin. Orthop. Relat. Res. 156 (1981) 240–247.
[19] A.J. van den Bogert, L. Read, B.M. Nigg, An analysis of hip joint loading during walking, running, and skiing, Med. Sci. Sport. Exerc. 31 (1) (1999) 131–142.
[20] S.H. Chen, M.C. Chiang, C.H. Hung, S.C. Lin, H.W. Chang, Finite element comparison of retrograde intramedullary nailing and locking plate fixation with/without an intramedullary allograft for distal femur fracture following total knee arthroplasty, Knee 21 (1) (2014) 224–231.
[21] K.J. Koval, F.J. Kummer, S. Bharam, D. Chen, S. Halder, Distal femoral fixation: a laboratory comparison of the 95 degrees plate, antegrade and retrograde inserted reamed intramedullary nails, J. Orthop. Trauma 10 (6) (1996) 378–382.
[22] H.H. Bayraktar, E.F. Morgan, G.L. Niebur, G.E. Morris, E.K. Wong, T.M. Keaveny, Comparison of the elastic and yield properties of human femoral trabecular and cortical bone tissue, J. Biomech. 37 (1) (2004) 27–35.
[23] J.W. Yang, K.H. Koo, M.C. Lee, P. Yang, M.D. Noh, S.Y. Kim, K.I. Kim, Y.C. Ha, M.S. Joun, Mechanics of femoral head osteonecrosis using three-dimensional finite element method, Arch. Orthop. Trauma Surg. 122 (2) (2002) 88–92.
[24] W.D. Leslie, S.L. Brennan-Olsen, S.N. Morin, L.M. Lix, Fracture prediction from repeat BMD measurements in clinical practice, Osteoporos. Int. 27 (1) (2016) 203–210.
[25] M. Srivastava, C. Deal, Osteoporosis in elderly: prevention and treatment, Clin Geriatr. Med. 18 (3) (2002) 529–555.
[26] M. Djurić, P. Milovanović, D. Djonić, A. Minić, M. Hahn, Morphological characteristics of the developing proximal femur: a biomechanical perspective, Srp. Arh. Celok. Lek. 140 (11–12) (2012) 738–745.

[27] E. Sensoz, F.M. Özkal, V. Acar, F. Cakir, Finite element analysis of the impact of screw insertion distal to the trochanter minor on the risk of iatrogenic subtrochanteric fracture, Proc. Inst. Mech. Eng. H 232 (8) (2018) 807–818.
[28] F. Chiba, Y. Makino, S. Torimitsu, A. Motomura, G. Inokuchi, N. Ishii, Y. Hoshioka, H. Abe, R. Yamaguchi, A. Sakuma, S. Nagasawa, H. Saito, D. Yajima, Y. Fukui, H. Iwase, Stature estimation based on femoral measurements in the modern Japanese population: a cadaveric study using multidetector computed tomography, Int. J. Leg. Med. 132 (5) (2018) 1485–1491.
[29] K.M. Flegal, Body mass index of healthy men compared with healthy women in the United States, Int. J. Obes 30 (2) (2005) 374–379 (Lond)..
[30] H.A. Bulaqi, M. Mousavi Mashhadi, H. Safari, M.M. Samandari, F. Geramipanah, Effect of increased crown height on stress distribution in short dental implant components and their surrounding bone: a finite element analysis, J. Prosthet. Dent. 113 (6) (2015) 548–557.
[31] F. Fraysse, R. Dumas, L. Cheze, X. Wang, Comparison of global and joint-to-joint methods for estimating the hip joint load and the muscle forces during walking, J. Biomech. 42 (14) (2009) 2357–2362.
[32] K.G. Faulkner, W.K. Wacker, H.S. Barden, C. Simonelli, P.K. Burke, S. Ragi, L. Del Rio, Femur strength index predicts hip fracture independent of bone density and hip axis length, Osteoporos. Int. 17 (4) (2006) 593–599.
[33] H. Li, Y. Wang, J.K. Oni, X. Qu, T. Li, Y. Zeng, F. Liu, Z. Zhu, The role of femoral neck anteversion in the development of osteoarthritis in dysplastic hips, Bone Jt. J. 96-B (12) (2014) 1586–1593.
[34] C.H. Turner, Bone strength: current concepts, Ann. N. Y. Acad. Sci. 1068 (2006) 429–446.
[35] K.C. Ng, G. Mantovani, M. Lamontagne, M.R. Labrosse, P.E. Beaulé, Increased hip stresses resulting from a cam deformity and decreased femoral neck-shaft angle during level walking, Clin. Orthop. Relat. Res. 475 (4) (2017) 998–1008.